

**PALEOMAGNETISM AND CYCLOSTRATIGRAPHY OF THE MIDDLE ORDOVICIAN KRIVOLUTSKY SUITE, KRIVAYA LUKA SECTION, SOUTHERN SIBERIAN PLATFORM: RECORD OF NON-SYNCHRONOUS NRM-COMPONENTS OR A NON-AXIAL GEOMAGNETIC FIELD?**

V.P. RODIONOV<sup>1</sup>, M.J. DEKKERS<sup>2</sup>, A.N. KHRAMOV<sup>1</sup>, E.L. GUREVICH<sup>1</sup>, W. KRIJGSMAN<sup>2</sup>,  
C.E. DUERMEIJER<sup>2</sup>, D. HESLOP<sup>2</sup>

- 1 VNIGRI, Laboratory of Paleomagnetism and Paleoreconstructions, Liteiny 39, 191104 St. Petersburg, Russia (paleomag@vnigri.spb.su)
- 2 Paleomagnetic Laboratory "Fort Hoofddijk", Utrecht University, Budapestlaan 17, 3584 CD Utrecht, Netherlands (dekkers@geo.uu.nl)

Received: July 30, 2002; Accepted: March 17, 2003

---

ABSTRACT

*The Middle Ordovician Volginsky and Kirensky fossil zones were sampled in the Krivaya Luka section (Krivolutsky suite) that outcrops along the Lena river in Siberia. The Volginsky and Kirensky zones are coeval to the Llandeilo in the global geologic time scale. The Krivaya Luka section consists of siltstones, clays, sandstones, and limestones, and displays a remarkably distinct sedimentary cyclicity, especially in its reddish middle part.*

*Stepwise thermal demagnetization yields three NRM components. Component A, isolated in the 100–250°C interval can be either normal or reversed. The normal A-component has a direction close to recent local magnetic field. The reversed A-component directions are scattered around a direction close to that of the lower Triassic Siberian traps. Component B, has unblocking temperatures that range from 400 to 500°C and is represented mainly by normal polarity directions. The B-component, isolated from rocks of the middle part of the section is of a normal polarity with  $D = 176.5^\circ$ ,  $I = 30.0^\circ$  and a North pole position at  $16.2^\circ\text{S}$ ,  $111.3^\circ\text{E}$ . The other parts of the section are characterized by intermediate B-directions, which resulted possibly by partially overlapping A- and C-components. The highest temperature dual-polarity component C was isolated in the 550–670°C interval, resulting in the detection of two complete polarity zones and three magnetic reversals. The C-component is characterized by the following mean directions: for the reversed component  $D = 335.7^\circ$ ,  $I = 6.9^\circ$ , and for the normal component  $D = 188.6^\circ$ ,  $I = 28.0^\circ$ , which is very close to the normal polarity directions of the B-component. The corresponding paleomagnetic North pole for reversed polarity rocks is  $32.6^\circ\text{S}$ ,  $137^\circ\text{E}$ , which is typical of Middle Ordovician rocks from Siberia – the mean pole for Llanvirn-Llandeilo is  $30^\circ\text{S}$ ,  $136^\circ\text{E}$  (cf. Smethurst et al., 1998) – whereas for normal polarity rocks the pole position  $17.2^\circ\text{S}$ ,  $99.1^\circ\text{E}$  is markedly different. Nevertheless, we assume that the C-component records the ancient geomagnetic field of Ordovician times, even though it does not pass the reversals test. This could be*

explained by overlapping *NRM* unblocking temperature spectra for the *B* and *C* components. In this case, the paleomagnetic pole positions should be interpreted with some caution.

In addition, the section was logged and sampled in detail for cyclostratigraphic purposes. Spectral analysis in the depth domain using the high-field susceptibility as input parameter showed that the observed cyclicity is most likely orbitally forced. Detected spectral peaks (significant at the 95% confidence level) were close to the expected positions of the periodicities of precession, obliquity and eccentricity for the Ordovician. Consequently, the average sediment accumulation rate is estimated at ~3.5 cm/kyr. Extrapolating this sedimentation rate yields a total duration of at least 1 Myr for the Volginsky fossil zone and 1.2 Myr for the entire Krivaya Luka section.

Keywords: palaeomagnetism, red beds, Middle Ordovician, Siberian Platform, magnetostratigraphy, cyclostratigraphy

## 1. INTRODUCTION

Palaeomagnetic investigations of Lower Palaeozoic rocks from the Siberian Platform were carried out since the early 1960s (e.g. *Khramov et al., 1965; Rodionov, 1966*). Apart from determination of paleomagnetic pole positions for Lower Palaeozoic rocks on the Siberian Platform, the recognition of magnetic polarity zones was a major goal of this early work. About 15–20 years later, the complete Lower Paleozoic magnetostratigraphy was delineated for the southern part of the platform (*Khramov and Rodionov, 1977; Khramov and Rodionov, 1980; Rodionov and Osipova, 1985*). The most suited sections were identified as standard sections, and primarily those were used for correlation to the global geologic time scale. A consistent and detailed magnetostratigraphic polarity (time) scale for the Lower Palaeozoic could be constructed (*Khramov et al., 1974*). The magnetic polarity patterns of the Ordovician fossil zones could be correlated over distances of more than 1000 km and a remarkable property of the primary component of the natural remanent magnetization (*NRM*) was noticed: in some stratigraphic intervals normal and reverse polarity directions in adjacent polarity zones appeared to be not entirely antipodal (*Torsvik et al., 1995; Iosifidi et al., 1999*). This observation required follow-up investigation to reveal whether the non-antipodality would be a property of the Ordovician geomagnetic field (*Pesonen and Halls, 1983*) or that the observed non-antipodality is the result of intricacies of *NRM* acquisition process and/or the *NRM* demagnetization behavior (*Khramov, 1988*). Recent investigations of the Middle Ordovician Krivolutsky suite in the stratotype and parastratotype areas have demonstrated this reversal asymmetry: differences in N–R directions range from 130° for the Volginsky zone to 164° for the Kirensky and Kudrinsky fossil zones. These values appear seemingly consistent over a distance of at least 500 km (*Pavlov et al., 1999; Rodionov et al., 2001*). However, the origin of the above-mentioned asymmetry could not be clarified.

In the present contribution we analyze in detail the *NRM* behaviour in the Krivolutsky suite where the asymmetry was reported to be highest. For our study, we selected the Krivaya Luka section (Fig. 1) which consists of grey and red colored rocks of the Volginsky and Kirensky fossil zones. Moreover, this section expresses a clear regular alternation of more and less indurated beds. These alternations are very similar to the

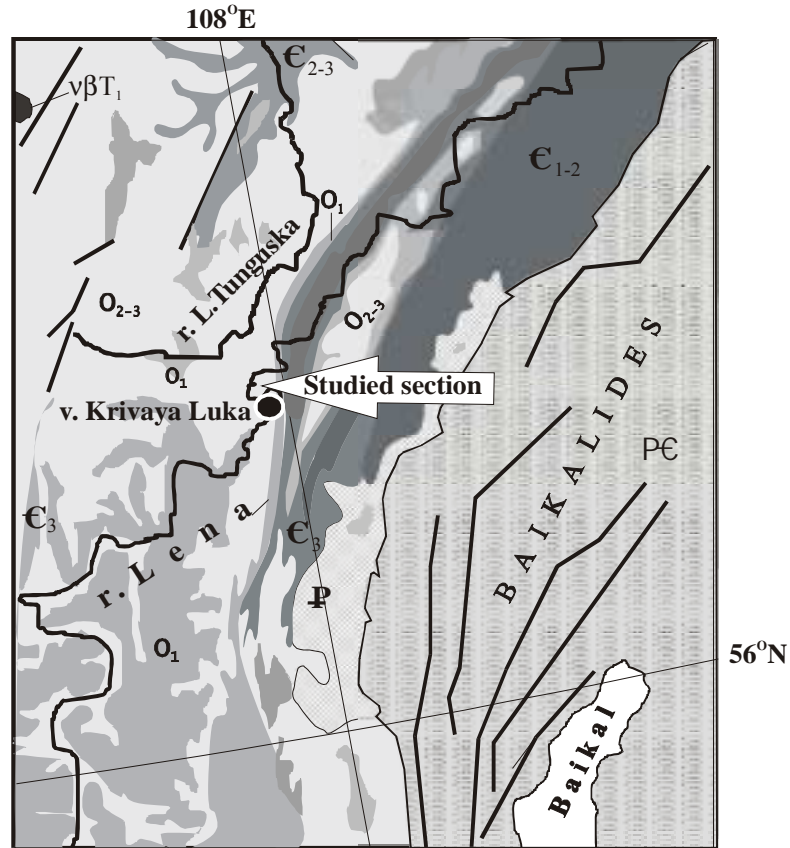


**Fig. 1.** Simplified geological map of Southern Siberian Platform. The sampling site is indicated with the black dot. Є = Cambrian with suffix 1 to 3 indicating old to young; O = Ordovician rocks (numbering referring to age division according to Cambrian rocks). P and PC = Precambrian units.

sedimentary cyclicality observed in Permian and Miocene red beds of France and Spain (Kruiver *et al.*, 2000; Krijgsman *et al.*, 1997), where it was proven to be related to changes in climate induced by the astronomical variations of the Earth's orbit. Therefore, we have undertaken an additional cyclostratigraphic sampling, focusing on the middle part of the section where the cyclic alternations are most distinct, to investigate a possible orbital forcing in the Ordovician sediments of the Siberian platform. This could provide important constraints on the duration of both the magnetic polarity zones and the fossil biozones, and enhance the resolution of magnetostratigraphic correlation.

## 2. GENERAL ORDOVICIAN STRATIGRAPHY IN THE LENA RIVER AREA

The subdivision of the south Siberian Ordovician formations and their correlation with the global geologic time scale are based on the rich invertebrate fauna. The lower

boundary of the Ordovician is somewhat arbitrary, but is defined at the top of the unfossiliferous variegated Verholensky and Ilginsky suites. Those suites are argued to be uppermost Cambrian of age (Nikiforova and Andreeva, 1961; Sokolov and Tesakov, 1975; Kanygin et al., 1977; Kanygin et al., 1989; Ogienko, 1992).

There are many good outcrops of Ordovician rocks along the Lena river and its tributaries. According to the accepted stratigraphic scheme (*Siberian Stratigraphic Resolution Committee, 1983*), which is based on the assemblages of brachiopodes, trilobites and conodonts, the Lower Ordovician is represented by the Ust-Kut suite of limestones, dolostones, and sandstones, overlain by argillaceous and calciferous sandstones, occasionally of red color. The thickness of this suite is ca. 100 m.

The Middle Ordovician of the river Lena region is represented by the Krivolutsky and Chertovsky suites, that are subdivided into the Mukhtinsky, Volginsky, Kirensko-Kudrinsky and Chertovsky zones. Stratotype sections of the Krivolutsky and Chertovsky suites are located along the Lena at 2 km downstream of the village of Kudrino. The parastratotype of the Krivolutsky suite is located c. 500 km downstream along the Lena near the village of Polovinka. The standard sequence of the suite starts with an intercalation of grey and variegated claystones and siltstones, overlain by variegated sandstones. Total thickness of the suite is 76 m. The youngest Middle Ordovician suite is the Chertovsky suite. It is represented by greenish-grey siltstones, overlain by variegated siltstones with thin layers of the limestones and sandstones. Thickness of this suite is 30 m.

The Upper Ordovician is represented by the Makarovsky suite; only the lower part of this suite is fossiliferous. Solely terrigenous red beds are developed here. The stratotype section of this suite is located along the Lena river, near the village of Makarovo where the thickness of this suite is 30 m. An unconformity separates Ordovician and Silurian strata in this region.

### 3. SAMPLING AND LABORATORY PROCEDURES

High-resolution palaeomagnetic sampling was carried out along a vertical profile across outcrops located close to the village of Krivaya Luka (57.6°N, 107.8°E; Fig. 1). Here, the Volginsky and Kirensky zones span a stratigraphic thickness of at least 42 m. Typically each 10–20 cm, an oriented hand sample was collected amounting to a total of 228 samples. The 228 oriented hand samples have been cut into 4 to 6 cubic specimens of 2 × 2 × 2 cm. Often one cube is thermally treated. Moreover, material for petrographic investigations was taken from the same hand samples.

Paleomagnetic analysis was done in the VNIGRI paleomagnetic laboratory (St. Petersburg, Russia) and in paleomagnetic laboratory “Fort Hoofddijk” (Utrecht, The Netherlands). Additional data were acquired in the paleomagnetic laboratory of the marine geophysics group of Bremen University (Germany). In St. Petersburg, the *NRM* intensity was measured on a JR4 spinner magnetometer (AGICO, Brno, Czech Republic, noise level c.  $5 \times 10^{-11}$  Am<sup>2</sup>). All samples were stepwise thermally demagnetized up to 670°C in a home-built non-magnetic furnace (residual field < 4–10 nT). An average of 14 demagnetization steps was carried out. The initial magnetic susceptibility was measured after each heating cycle using a KLY-2 susceptometer. To determine the *NRM*

components, principal component analysis (*Kirschvink, 1980*) was performed and precision of the directions calculated with the *Kent et al. (1983)* algorithm. On non-oriented samples, the *NRM* was also demagnetized with alternating fields with an automated 2G SQUID magnetometer (noise level  $3 \times 10^{-12}$  Am<sup>2</sup>) at Bremen University. This was done to tie the properties of the *NRM* during AF demagnetization to the properties during thermal demagnetization.

In addition, acquisition curves of the anhysteretic remanent magnetization (*ARM*) and isothermal remanent magnetization (*IRM*) were determined with the automated SQUID magnetometer at Bremen. Here, to support our paleomagnetic interpretation, we show a few examples only for reasons of brevity; a full account on the rock magnetic data will be given in a future contribution.

For cyclostratigraphic purposes a more detailed sample set was collected and a dedicated cyclostratigraphic logging was performed. It is known that the precession and obliquity periods change slowly with geological time while the eccentricity periods remain unchanged. *Berger et al. (1992)* calculated the dominant frequencies in orbital periods back to 500 Ma: in the Cambrian precessional periods are 16 and 18.7 kyrs and that for obliquity 29 (compare to 19 and 23 kyrs for present-day precession and 41 kyrs for present-day obliquity). To test for astronomically forced periods with spectral analysis techniques along the lines explained in *Kruiver et al. (2000)*, one needs approximately 7 samples per inferred cycle for the highest frequency to be tested. To test for a precessional origin of the basic cyclicity in the Krivaya Luka section implied at least one sample per ~9–10 cm. To test for an eccentricity origin of the basic cycle (sedimentation rate c. 6–7 times lower), three cycles were sampled quasi continuously (in total ~95 samples).

For all samples, the low-field susceptibility was measured with a KLY-2 susceptometer (AGICO, noise level  $4 \times 10^{-8}$  SI; typical sample values were at least three orders of magnitude higher), while the high-field susceptibility was obtained from the slope of the hysteresis loops between 0.5 and 1.0 Tesla, measured using an alternating gradient magnetometer (AGM) MicroMag2900 Model (Princeton, USA, noise level  $1 \times 10^{-9}$  Am<sup>2</sup>; typical sample values were at least three orders of magnitude higher). In rocks that contain remagnetized *NRM* components residing in a magnetite-like mineral (that has very high susceptibility values), the low-field susceptibility is somewhat suspect. In those cases, the low-field susceptibility that is quickly dominated by the magnetite contribution represents mixed geological ages. A secondary *NRM* component with a maximum unblocking temperature of 550°C is present in the Krivaya Luka section. At the same time the magnetic mineralogy consists of widely varying contributions of magnetite (*sensu lato*) and hematite as indicated by rock-magnetic analysis (cf. Fig. 3). These two aspects make the low-field susceptibility unsuited for spectral analysis of the Krivaya Luka section: variability could erroneously be interpreted along the lines of a changing magnetite input inferred to be climatic origin while it represents an unknown blend of later magnetite and changes in magnetite/hematite ratios that may have in part an other origin than a strict climatic one. To exclude a possible bias in the low-field susceptibility values that represent a variable contribution of ferrimagnetic and paramagnetic plus diamagnetic material, spectral analysis was focussed on the high field susceptibility. Changes in the high-field susceptibility are related to changes in the amount of paramagnetic minerals,

for example a changing clay mineral content or a changing provenance area. Such-like changes are comparatively straightforwardly related to climatic changes that have been shown in many cases to be orbitally forced in younger sediments.

## 4. RESULTS

### 4.1. *NRM* behaviour during thermal demagnetization

Magnetic properties of the red and grey rocks of the Krivaya Luka section appear to be very different. The mean value of the *NRM* for the red beds is 10 mA/m, whereas for grey colored rocks this value is 1 mA/m. Typical values of the magnetic susceptibility range from  $2.5$  to  $5.8 \times 10^{-4}$  for the red beds and from  $1.0$  to  $3.0 \times 10^{-4}$  SI-units for the grey rocks respectively. During thermal demagnetization of the red rocks the susceptibility remained stable or decreased only slightly up to temperatures of c.  $500^\circ\text{C}$ . At higher temperatures it started increasing. Generally, the susceptibility in the grey rocks started increasing at lower temperatures, from  $350$ – $400^\circ\text{C}$  upward. When the susceptibility increased the quality of the *NRM* demagnetization diagrams deteriorated slightly as one would expect. In most cases, however, components could still be reliably determined. Thermal demagnetization experiments permit us to isolate two different groups of samples, according to their unblocking temperature spectra. The first group is characterized by rather wide unblocking temperature spectra, with the main body of their unblocking occurring in the range  $T_{ub} = 350$ – $500^\circ\text{C}$  (Fig. 2; 94, 95, 103, 106, 109). A second group can be distinguished with maximum unblocking temperatures  $T_{ub}$  ranging from  $550$ – $670^\circ\text{C}$  (Fig. 2; 123, 124, 149N).

Zijderveld diagrams show that in each group two or three *NRM* components with different directions are isolated in different temperature intervals (Fig. 2; 103, 123). The component with lowest unblocking temperatures ( $T_{ub}$ ), with  $T_{ub}$  between  $100$  and  $250^\circ\text{C}$ , labelled A, can be either normal or reversed. The normal A component has a direction close to that of the recent local geomagnetic field and is interpreted to be of viscous origin (Fig. 2; 94, 95). The reversed A-component directions are scattered and have a mean direction close to that of the Lower Triassic Siberian traps. The scattered nature, however, precludes any geologic interpretation. The reversed A-component directions are occasionally close to the directions of the B-component (Fig. 2; 109). Those samples are considered to be completely overprinted.

The directions of the B component with  $T_{ub}$  ranging from  $300$  to  $500^\circ\text{C}$ , are divided into two groups characterized either by southern or by (somewhat scattered) northern directions. The northerly directions are especially typical for cases, when the B component is the final distinguishable component (Fig. 2; 94, 95 106). These B directions are compatible with directions typical of Ordovician times for the region.

The C component has high unblocking temperatures, with  $T_{ub}$  ranging from  $550$  to  $670^\circ\text{C}$ , implying that it is residing in hematite (Fig. 2; 123, 124, 149N). Component C is of dual polarity and has directions typical of Middle Ordovician rocks of the Siberian Platform. Therefore it is considered a primary *NRM* component enabling a magnetostratigraphic interpretation. In many cases, especially where B- and C-component directions are not so different,  $T_{ub}$  - spectra for these components appear to overlap. In rare cases, due to the large noise at high- temperatures, mean Fisher directions, calculated

for temperatures close to the Curie points for magnetite (for the B component) and for hematite (for the C component) have been used.

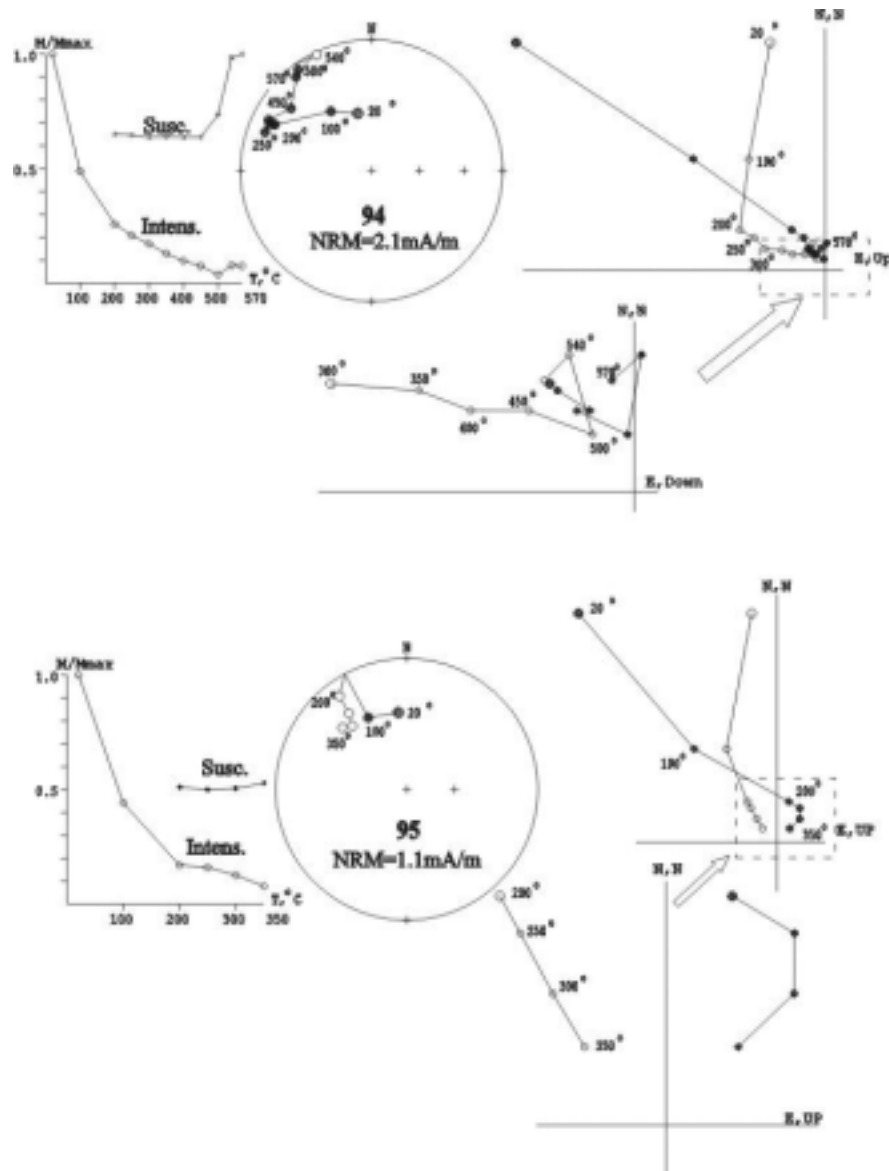


**Fig. 2.** Zijderveld diagrams, equal area plots, and decay curves of selected samples. The behaviour of the low-field susceptibility during thermal demagnetization is indicated as well.

4.2. *NRM* properties during AF demagnetization

AF demagnetization of the *NRM* was performed on non-oriented samples to compare the properties of the *ARM* and *IRM* acquisition curves to features measured during AF demagnetization on the same specimens. The alternating field properties appeared to be difficult to interpret. Most samples showed a marked decay during AF demagnetization steps up to 20 mT. At fields higher than 40–50 mT about 30% of the samples showed erratic demagnetization behaviour. Red rocks could not be demagnetized completely in

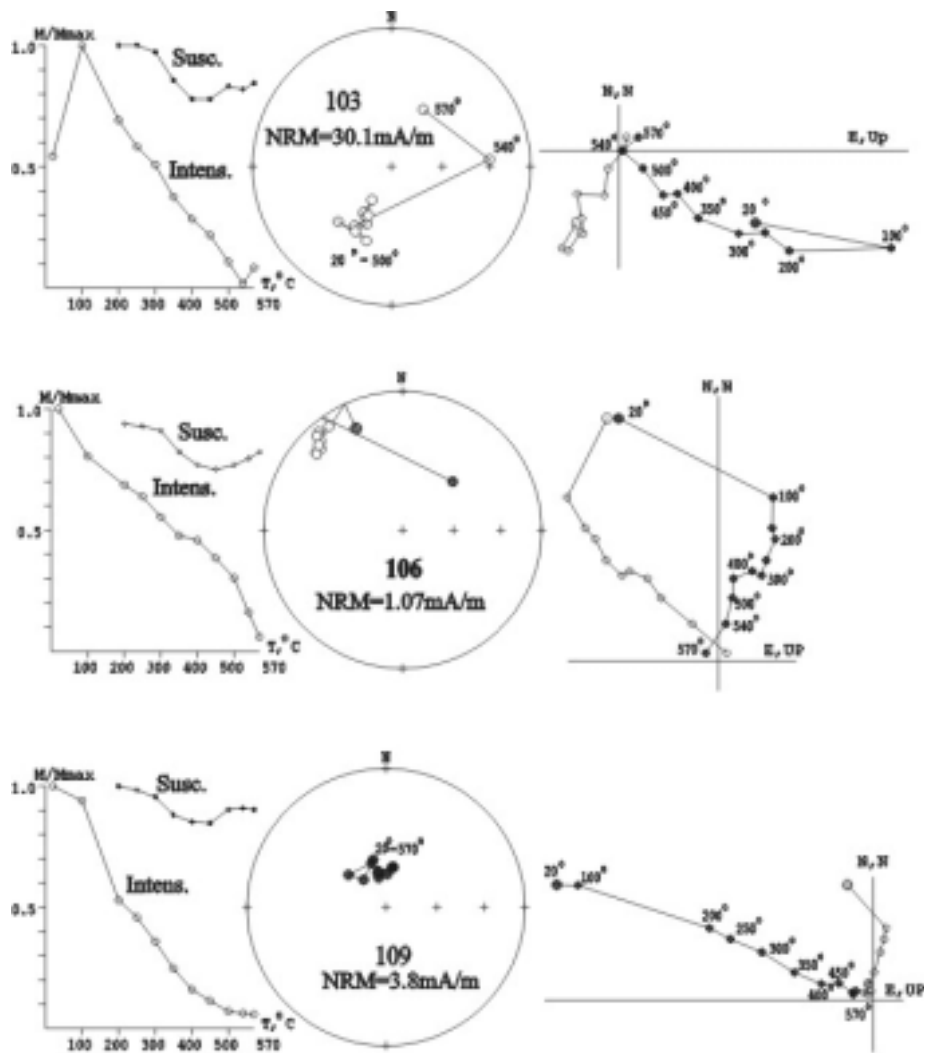
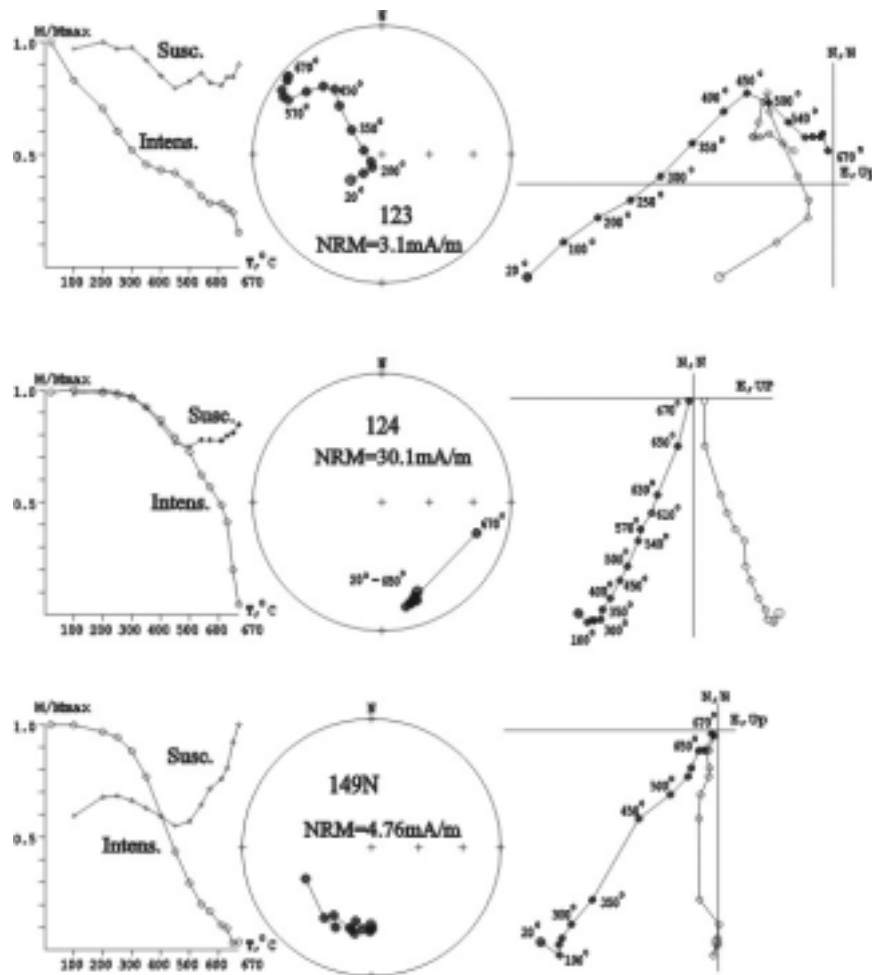
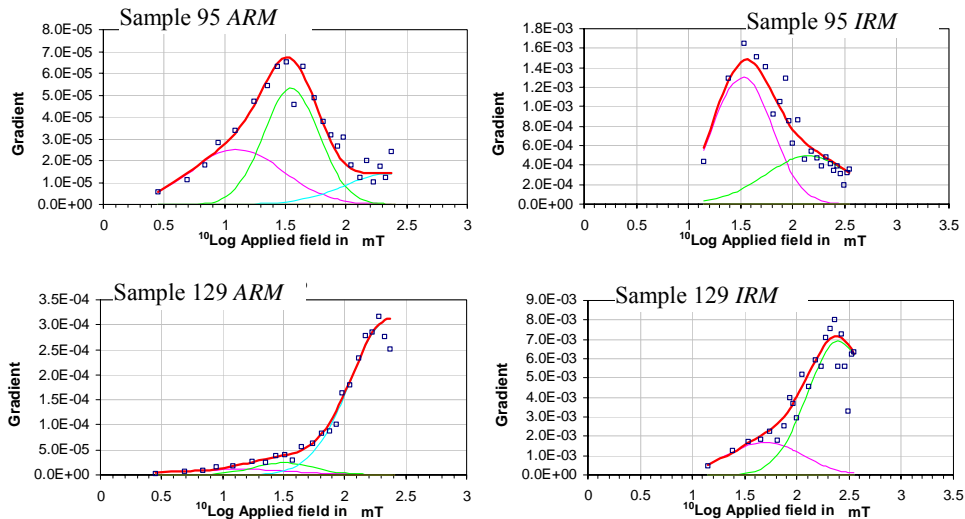


Fig. 2. Continuation.

the 160 mT maximum AF available and showed univectorial decay toward the origin. Therefore only thermal data were considered for the interpretation of the *NRM*. In some grey rock samples, components between 40 and 80 and/or between 100 and 160 mT could be distinguished. In those samples thermal demagnetization yielded important remagnetized components. Consequently, remagnetization is apparently mostly confined to low-coercivity components that can be AF demagnetized. Thus, magnetite or slightly cation-deficient magnetite with very a high specific low-field susceptibility presumably are the carriers of those components. This supports our doubt on the suitability of the low-field susceptibility for spectral analysis. Instead, only high-field susceptibility data were processed.



**Fig. 2.** Continuation.



**Fig. 3.** Gradient acquisition plots (GAP) of two samples (grey lithology), showing the markedly different behaviour of their ARM and IRM. For the ARM three components were required for an optimal fit, for the IRM only two. In sample 95, the low-coercivity component of the ARM represents 35% of the total ARM ( $5.05 \times 10^{-6} \text{ Am}^2/\text{kg}$ ), the intermediate component 45%, and the high-coercivity ARM 20%. For sample 129 these values are 4, 5, and 91% respectively (total ARM is  $24.55 \times 10^{-6} \text{ Am}^2/\text{kg}$ ). In sample 95 the low-coercivity component represents 64% of the total IRM ( $1.07 \times 10^{-4} \text{ Am}^2/\text{kg}$ ); in sample 129 it is 22% of the total IRM ( $5.67 \times 10^{-4} \text{ Am}^2/\text{kg}$ ).

#### 4.3. Rock magnetic measurements

ARM and IRM acquisition curves were determined for all samples. As an example, ARM and IRM component fitting (Kruiver et al., 2001; Heslop et al., 2002) are shown for samples 95 and 129 (Fig. 3). ARM isolates two components in the low-field range (with  $B_{1/2}$  of  $\sim 13$  and  $\sim 35$  mT) and IRM only one component ( $B_{1/2} \sim 50$  mT). This difference is also observed by Kruiver et al. (2002) and is related to the amount of data points that is much larger for the ARM in low fields. The third ARM component and the second IRM component seem to be similar. Obtained values are comparatively low for 'standard' hematite. The intensities of the ARM and IRM components vary substantially through the section, also among samples with seemingly similar lithology. The variability in ARM properties could be related to the viscous part of the NRM behaviour. A full account of the variability in magnetic properties is intended to be presented in a future publication.

The observed wide variability in low-coercivity properties prompted us to focus on the high-field susceptibility for spectral analysis. The low-coercivity components are saturated above  $\sim 0.3$ – $0.4$  Tesla. Hence, variability in the high-field susceptibility determined from the slope in hysteresis loops is not biased by the presence of low-coercivity components. The high field slope indicates the variation in paramagnetic mineral content, i.e. the silicates present in the rocks. For the rocks under investigation the variability most likely derives from changes in clay mineral abundance and composition,

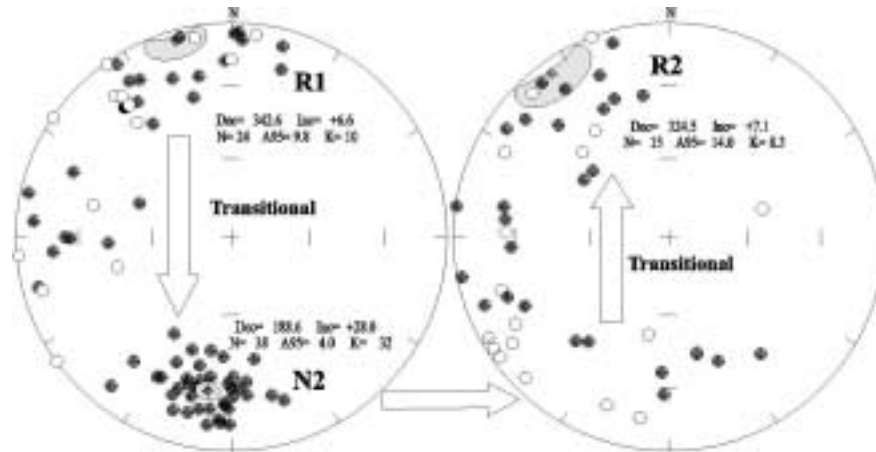


**Fig. 4.** Stereoplots of the sample mean paleomagnetic directions of the characteristic component. The lowermost N1 zone is not considered due to its low number of samples. Also the transition to the reverse R1 zone is sharp, no transitional directions were measured.

properties that have been shown to be related to climate changes for example in Neogene sediments (e.g. *Foucault and Mélières, 2000*). Hence, the high field susceptibility may show orbital frequencies. It should be mentioned that hematite is not entirely saturated as well in the field range adopted. However, hematite has a high-field susceptibility comparable to many paramagnetic silicates. So, variations in hematite content will only influence the high-field susceptibility to a very minor extent (estimation less than 5%). Measured variation was much more.

## 5. DISCUSSION

### 5.1. Magnetostratigraphy and paleomagnetic pole positions

The characteristic remanent magnetization (*ChRM*) component, component C, forms two directional clusters with shallow inclinations that project in stratigraphic coordinates in the southern and north-western parts of equal area plots (Fig. 4). A diffuse zone of intermediate directions occurs as well. This testifies that it is not possible to discern a reliable C component in all samples. Plotted in stratigraphic order four polarity intervals can be distinguished, from the bottom of the sampled section to ~1 m, from ~1 m to ~16 m, from ~16 m to ~31 m, and from ~31 m to 42 m, the top of the analyzed section (Fig. 5). The intervals of normal polarity are labelled N1 and N2 and those of reversed polarity R1 and R2 respectively. The polarity zonation is based on the calculation of the “deviation” angle between the sample direction and mean direction for the N2 zone. The N2 zone was chosen for this purpose because it showed the best directional grouping. The samples with intermediate directions form distinct levels bordering the individual polarity zones (Fig. 5). Both boundaries of the N2 zone are poorly defined. Hatched zones where intermediate directions dominate are 2.5 to 3 m thick respectively. This precludes a firm

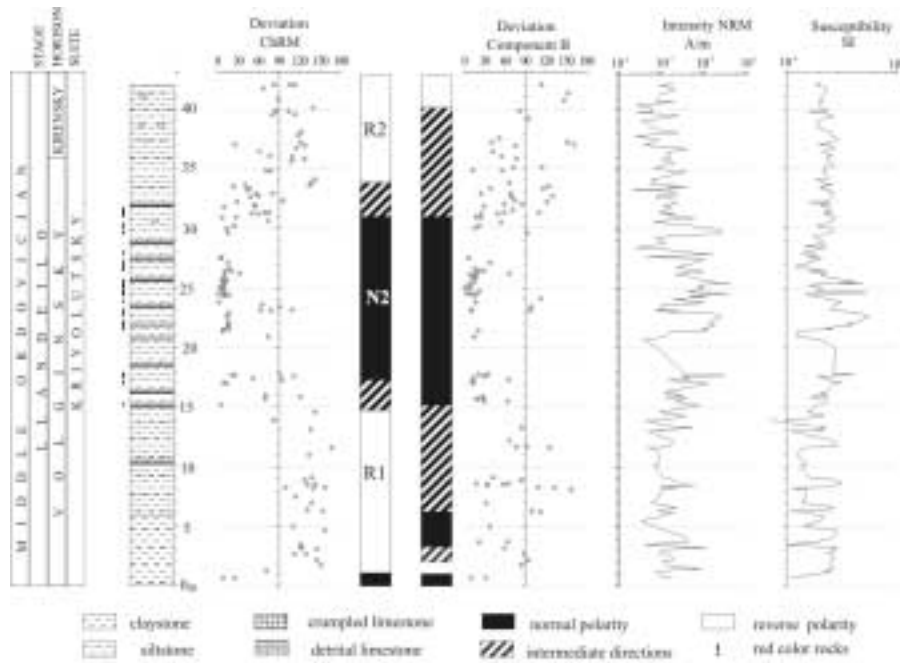


Fig. 5. Summary magnetostratigraphy for the *ChRM* and B components.

establishment of the length of the polarity zones. It is emphasized that the reversed polarity zones R1 and R2 as delineated by the C component, are associated with grey colored rocks. In contrast, red beds dominate the central part of the section with the thick normal polarity zone N2.

The B-component is treated along the same lines as the C-component (Fig. 5). It shows a polarity pattern completely different from that of the C-component: normal polarities and transitional directions prevail. B-component directions have been mainly obtained using the remagnetization circles intersection technique. These are close to directly isolated directions from rocks of the central part of the section where  $D = 176.5^\circ$ ,  $I = 30.0^\circ$ , ( $K = 32.0$ ,  $\alpha_{95} = 3.9^\circ$ ,  $N = 41$ ;  $K$  and  $\alpha_{95}$  are the Fisher parameters and  $N$  the number of samples, cf. Fig. 6). Mean directions and statistics for the B and C components are compiled in Table 1.

North pole positions for the lower and upper parts of section (R1 and R2 zones) are  $34.1^\circ\text{S}$ ,  $128.9^\circ\text{E}$ , with semi axes of the uncertainty oval  $dp = 5.1^\circ$ ,  $dm = 10.0^\circ$  and  $29.2^\circ\text{S}$ ,  $149.4^\circ\text{E}$  ( $dp = 4.2^\circ$ ,  $dm = 8.4^\circ$ ) respectively. For both sets lumped together, the pole position is  $32.6^\circ\text{N}$ ,  $137.0^\circ\text{E}$  ( $dp = 4.2^\circ$ ,  $dm = 8.3^\circ$ ). Their confidence ovals overlap. The B component that is determined without the remagnetization circles technique yields a pole position at  $16.2^\circ\text{S}$ ,  $111.3^\circ\text{E}$  ( $dp = 2.4^\circ$ ,  $dm = 4.3^\circ$ ).

**Table 1.** Average directions for the *NRM* components.

| Polarity Zone     | Component B |       | Component C |       | R1+R2 |
|-------------------|-------------|-------|-------------|-------|-------|
|                   | N           | R1    | N2          | R2    |       |
| <i>D</i> [°]      | 163.7       | 342.6 | 188.6       | 324.5 | 335.7 |
| <i>I</i> [°]      | 15.1        | 6.6   | 28.0        | 7.1   | 6.9   |
| <i>N</i>          | 33          | 24    | 38          | 15.0  | 39    |
| <i>k</i>          | 14.2        | 9.8   | 32.0        | 8.4   | 8.6   |
| $\alpha_{95}$ [ ] | 6.9         | 10.0  | 4.0         | 14.0  | 8.3   |

## 5.2. Cyclostratigraphy

A dedicated cyclostratigraphic sampling was carried out from level 22 m to 48 m. The lowermost and topmost parts of the section were less suited for the analysis of cycles because of outcrop quality. Hysteresis loops were measured for all samples that served to derive the high-field susceptibility. In Fig. 7a the input series is presented with the dotted line. The data were processed with the Monte Carlo version of the CLEAN algorithm (Roberts *et al.*, 1987; Heslop and Dekkers, 2002) that is designed for calculating spectra of unequally spaced data series. Spectral analysis was done in the depth domain. With the criteria of no hiatuses (also needed for meaningful magnetostratigraphy) and a constant sedimentation rate this is equivalent to the time domain. It is noted here that with the procedure adopted no tuning or assumptions concerning the sedimentation rate are required. The section appeared to be continuous from visual inspection of the outcrop. Also evolutive spectral analysis (using the same Monte Carlo CLEAN software) indicated stable spectral peaks, so a constant sedimentation rate for the peridocities at hand. If the sedimentation rate would have varied in an erratic sense no spectral peaks would have resulted.

The spectra were processed with 10% white noise addition. This is equivalent to the amount of variation of the high-field susceptibility in the “base-level”, i.e. with the exclusion of three very high data points (Fig. 7a). White noise was chosen because the number of data points (~280) is comparatively small and because the spectra did not show a red noise appearance (with a noise level going up in the very low frequency part of the spectrum). In the Monte Carlo simulation, each individual spectrum was iterated 500 times (CLEANed) with a CLEAN factor *g* of 0.1 (the recommended value); this procedure was repeated 1000 times, each time with a new white noise array added to the input data.

The resulting spectrum is shown in Fig. 7b. The peaks that are significant at the 95% confidence level occur at frequencies of 0.0023, 0.0103, 0.01613, and 0.01758  $\text{cm}^{-1}$ . The two peaks at lower frequencies than 0.0023 are not taken into consideration because not enough periods are present in the spectrum. The observed frequencies in the depth domain can now be transformed to the time domain by assigning a duration for a specific peak. Ideally, the template of Ordovician orbital frequencies (Berger *et al.*, 1992; see Table 2) should be found at the expected frequencies in the depth domain, if the observed

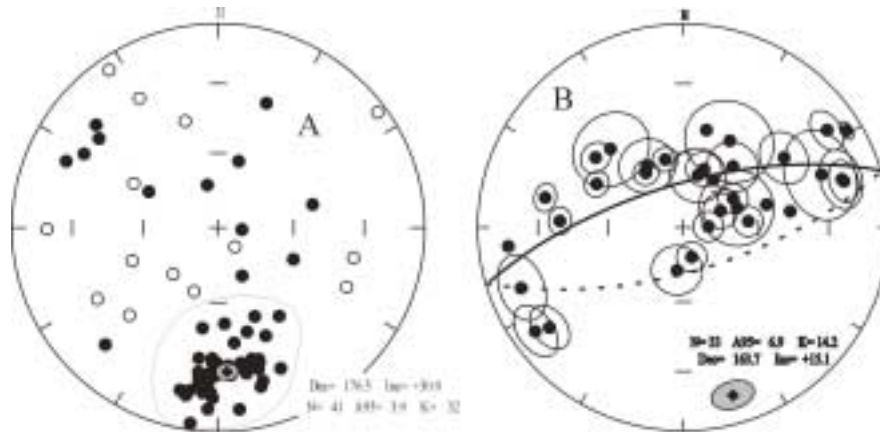


**Fig. 6.** (A) Stereoplot of the paleomagnetic directions of the B component and the mean direction (with cone of confidence at the 95% level) for the selected samples. (B) Poles of demagnetization circles for the intermediate temperatures. The overall pole plots close to the direction calculated in (A).

periodicity is indeed orbitally forced. *Kruiver et al. (2000)* found Permian orbital periodicity in a red bed section in Southeastern France with the same procedure. If the significant peak at  $0.0023 \text{ cm}^{-1}$  is assigned to be the eccentricity peak with a period of 125 kyr, the other frequencies correspond to periods for 27.9 kyr for the obliquity peak, and 17.82 and 16.35 kyr for the two precession peaks. This is at most only 1 kyr off the expected frequencies for the obliquity peak and the two precession peaks for Ordovician/Cambrian times (cf. Table 2), a remarkable result seen in the light of the uncertain factors in the whole procedure. Similar offsets are not uncommon in modern sediments. Support of assigning 125 kyr and not the “classical” 100 kyr to the peak at  $0.0023 \text{ cm}^{-1}$  is also given by the appearance of the 95 kyr peak (that is present in the eccentricity band as well) at the expected frequency with a significance only slightly less than 95%. Also in modern sedimentary sequences the dominant periodicity in eccentricity can vary along similar lines (e.g. *Berger, 1984*). It is also very remarkable that only orbital frequencies – and not a single other frequency – are significant at the 95% level. It is therefore likely that observed variability is indeed orbitally forced.

The stability of the spectral peaks was tested by evolutive spectral analysis (using the same Monte Carlo CLEAN software) by cutting the section in two halves and moving in one-meter segments through the section (thus in the depth domain). The spectral peaks appeared to be stable with respect to their position and remained significant at the 95% level (the relative heights varied), yielding evidence for the constant sedimentation rate condition. A portion of the section where cyclicity was judged to be most apparent in the field, was sampled with a very close sample spacing (2–3 cm resolution) to test for the interpretation that the cyclicity would represent eccentricity and not precession. Running the spectral analysis on this high-resolution data set did not show any meaningful orbital frequencies (at any significance level, no sense could be made from observed periodicity).

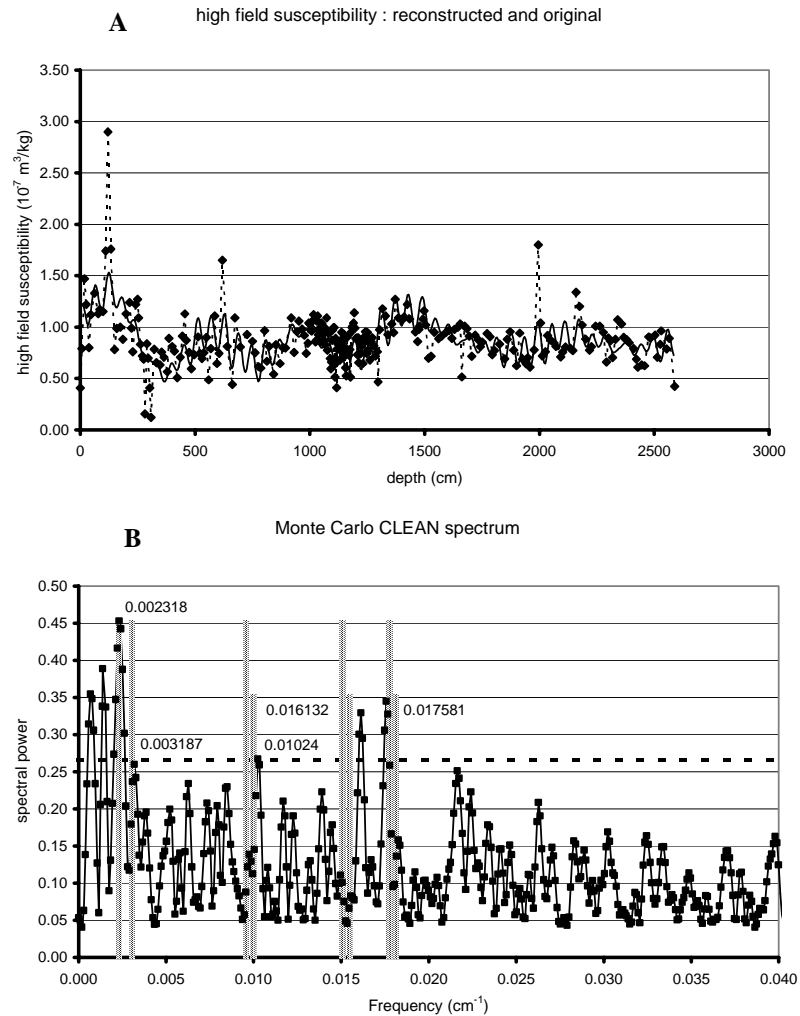


**Fig. 7.** (A) Input high-field susceptibility as a function of stratigraphic level (dotted line with solid squares indicating actual data points) and reconstructed signal from the spectral peaks that are significant at the 95% level (thin solid line). (B) Monte Carlo CLEAN spectrum. The horizontal line indicates the 95% significance level. Expected frequencies for obliquity and precession in Ordovician and Cambrian times (long and short hatched bars respectively) when assigning the eccentricity at  $0.0023 \text{ cm}^{-1} 125 \text{ kyr}$  are indicated.

So, the line of reasoning that the periodicity ascribed to precession would be in reality representing eccentricity cannot hold because no peaks show up at the expected higher frequencies (of obliquity and precession). This provides supporting evidence for the interpretation made in the foregoing.

**Table 2.** Orbital periodicities in the Ordovician and Cambrium (after Berger et al., 1992).

| Age | Precession 1<br>[kyr] | Precession 2<br>[kyr] | Obliquity 1<br>[kyr] | Obliquity 2<br>[kyr] |
|-----|-----------------------|-----------------------|----------------------|----------------------|
| 0   | 19                    | 23                    | 41                   | 54                   |
| 400 | 16.7                  | 19.7                  | 31.6                 | 38.7                 |
| 450 | 16.3                  | 19.2                  | 30.3                 | 36.8                 |
| 500 | 16.0                  | 18.7                  | 29.0                 | 35.0                 |

Periodicities are calculated under the assumption of a constant eccentricity of 100 kyr. In reality there is spectral power at 100 kyr and 125 kyr that varies through time. Obliquity 2 has much weaker spectral power than Obliquity 1.

The astronomical origin of the sedimentary cyclicity in the Krivaya Luka section provides a unique opportunity to independently derive reliable constraints on the duration of individual polarity zones and fossil biozones. Under the assumption that the significant peak at  $0.0023 \text{ cm}^{-1}$  can indeed be assigned to be the eccentricity peak with a period of 125 kyr, the average sedimentation rate in the Krivaya Luka section can be estimated at  $\sim 3.5 \text{ cm/kyr}$ . Extrapolating this sedimentation rate yields a total duration of at least 1 Myr for the Volginsky fossil zone and approximately 1.2 Myr for the entire Krivaya Luka section. The duration of the two complete polarity zones is comparable to that of polarity zones of Tertiary age. The duration of mixed/undefined polarity intervals is rather long but also in much younger rocks the recording of polarity transitions can be complex. In the detailed coercivity analysis that is currently being carried out, those intervals and the neighbouring stable polarity levels get special focus.

### 5.3. Field tests

The possibilities to apply field tests are very restricted in the case of the Ordovician sedimentary rocks outcropping along the Lena river. Horizontal bedding and the absence of within-formation conglomerates excluded the fold- and conglomerate tests. The reversals test, applied for part of the Ordovician section investigated in the Krivaya Luka section is negative, but it seems not to be the result of the secondary origin of the *NRM*-components isolated (see below). It is very important that the N2 zone traces the same stratigraphic position over a distance of 500 km (Rodionov, Osipova 1985; Rodionov et al, 2001). Hence, our result for Krivaya Luka passes the stratigraphic test.

### 5.4. Non-antipodality of the normal and reversed C-components

The intermediate temperature B-component has mostly a normal polarity. Only six levels in the grey-colored rocks show a normal C-component direction that is close to the C-component direction extracted from the red beds. This means that the C-component of both red and grey rocks records geomagnetic field of the time rather close to the early stages of rock formation. On the other hand, all of the above mentioned mean directions, both for C- and B-components, do not pass the reversals test. Deviations from antipodality

reach up to 40°, mainly due to clockwise rotation of directions for the N2 zone, relative to typical Middle Ordovician directions for the South of the Siberian platform. Two alternative hypotheses for the origin of this observation may be proposed:

The long reversed polarity interval during middle Ordovician times was followed by an interval of a “transitional” field configuration with marked non-axial and non-dipole components. Hence, the R1 → N2 reversal could be considered to have been incomplete. Although it cannot be ruled out completely, prolonged incompleteness of a reversal is unlikely because it has not been observed for reversals of younger age. A persistent measurable octupole field component that would vary slightly with time, has recently been proposed for the geomagnetic field (Kent and Smethurst, 1998; Van der Voo and Torsvik, 2001). Non-antipodality of normal and reversed directions could then be caused if the dipole component and octupole component of the field would behave independently during a reversal (for example one could reverse and the other not). The possibility of a persistent octupole field component is presently hotly debated. In addition, there are no firm indications why – if present at all – an octupole would indeed behave independent of the dominant dipole. Seeking a geomagnetic origin to explain the non-antipodality of normal and reverse directions would require high-quality data to rule out other explanations.

The multicomponent *NRM* in these rocks represents different times of acquisition. As a result the *NRM* components recorded fields of normal and reverse polarity (and may be even transitional), with ages that may range up to Silurian age. The demagnetization behaviour is therefore complex and overlapping tails in unblocking temperature spectra may cause non-antipodality between normal and reverse paleomagnetic directions. An example of such behaviour are the upper Cretaceous rocks analyzed by Groot *et al.* (1989), the observed substantial non-antipodality is explained by subtleties in the demagnetization behaviour of those samples and no major non-dipole contribution of the geomagnetic field is invoked.

Presently we regard the 2<sup>nd</sup> hypothesis which is similar to that proposed by Iosifidi *et al.* (1999), more likely for the following reasons. (1) The behaviour of the high-temperature C-component in the N2 polarity zone is complex. When the *NRM* contains only one directional component, i.e. B- and C-components have the same direction, the mean direction characterized by:  $D = 173^\circ$ ,  $I = 29.8^\circ$  ( $K = 86$ ,  $\alpha_{95} = 6.0^\circ$ ,  $N = 8$ ), which yields a typical Middle Ordovician pole  $\Phi = -16.2^\circ$ ,  $\Lambda = 114.8^\circ$ ,  $dp = 3.7^\circ$ ,  $dm = 6.6^\circ$ . In contrast, when the *NRM* is a vectorial sum of different B- and C-components, the mean direction for C-component is rotated clockwise, while the B-component direction lies close to the direction of the C-component for single-component specimens. Two-component *NRM* is documented in both grey and red-colored rocks. B-components, isolated in the rocks from the two reversed polarity zones (evidently based on the behaviour of the C-component) have a normal polarity with the above mentioned mean direction  $D = 176.5^\circ$ ,  $I = 30.0^\circ$  ( $K = 32.0$ ,  $\alpha_{95} = 3.9^\circ$ ,  $N = 41$ ). During thermal demagnetization of those specimens from the N2 zone, which yield “rotated” *NRM*-components, it is possible to track movements of directions along the great circle approximately clockwise toward the reverse directions, or anticlockwise toward the normal directions, typical of the Middle Ordovician on the Siberian Platform. This implies that “rotated” normal directions are the result of a superposition of N- and R-directions,

that are not exactly antipodal. Hence, it is most likely that single-component *NRM*s and the B-component of the two-component *NRM*s are primary components within the normal polarity zones, whereas the B-component with a normal polarity within reverse polarity zones is secondary. Intermediate B-directions result from the superposition of the normal and reversed components, which are not exactly antipodal; their relative input would determine the position of each of these intermediate directions. Possible mineralogical reasons for this are currently being investigated.

## 6. CONCLUSIONS

The rocks analyzed here showed a complex *NRM* behaviour with three, in part overlapping *NRM* components. Nonetheless it was possible to isolate a characteristic *NRM* component of dual polarity of Ordovician age in the section. With the help of cyclostratigraphy, constraints can be put on the duration of individual polarity zones, enhancing the value of magnetostratigraphy as a correlation tool. The present data seem to indicate that there may be causal relations between *NRM* component behaviour and lithology in the Krivaya Luka section. This clearly is the case between the red beds on the one hand and the greyish lithology on the other. To further substantiate possible underlying relations between *NRM* components and lithological intricacies a detailed coercivity analysis is being carried out that forms the topic of a future contribution.

*Acknowledgements:* We thank Piet Jan Verplak for measuring the hysteresis loops and Tom Mullender for his help during their processing. M.J.D. acknowledges the Bremen marine magnetism group for their hospitality and support during part of his sabbatical leave. These investigations have been supported by the INTAS programme created by the European Union (INTAS project 99-01273).

## References

- Berger A., 1984. Accuracy and frequency stability of the Earth's orbital elements during the Quaternary. In: Berger A., Imbire J., Hays J., Kukla G. and Salzman B. (eds.), *Milankovitch and Climate. NATO ASI Ser. C*, **126**, 3–39.
- Berger A., Loutre M.F. and Laskar J., 1992. Stability of astronomical frequencies over the Earth's history for paleoclimate studies. *Science*, **255**, 560–566.
- Foucault A. and Mélières F., 2000. Palaeoclimatic cyclicity in central Mediterranean Pliocene sediments: the mineralogical signal. *Palaeogeogr. Palaeoclim. Palaeoecol.*, **158**, 311–323.
- Groot J.J., de Jonge R.B.G., Langereis C.G., ten Kate G.H.Z. and Smit J., 1989. Magnetostratigraphy of the Cretaceous-Tertiary boundary at Agost (Spain). *Earth Planet. Sci. Lett.*, **94**, 385–397.
- Heslop D. and Dekkers M.J., 2002. Spectral analysis of unevenly spaced climatic time series using CLEAN: signal recovery and derivation of significance levels using a Monte Carlo simulation. *Phys. Earth Planet. Inter.*, **130**, 103–116.
- Heslop D., Dekkers M.J., Kruiver P.P. and van Oorschot I.H.M., 2002. Analysis of isothermal remanent magnetisation acquisition curves using the expectation-maximisation algorithm. *Geophys. J. Int.*, **148**, 58–64.

*Paleomagnetism and Cyclostratigraphy of a Middle Ordovician Section in Siberia*

- Iosifidi A.G., Khranov A.N., Rodionov V.P., Pisarevsky S.A. and Popov V.V., 1999. Geomagnetic reversals in the Early Paleozoic: 2. A nonsynchronous record of Middle Ordovician reversals in the Berezovskaya section, southern Siberian Platform. *Physics of the Solid Earth*, **35**, 24–32.
- Kanygin A.V., Moskalenko A.G., Jadrenkina A.G., Abaimova G.P., Semenova V.S., Sychev O.V. and Timokhin A.V., 1989. *Ordovician of Siberian Platform. Fauna and Stratigraphy of Lena Facial Zone (Ordovik sibirskoi platformy. Fauna I stratigrafija Lenskoi fazial'noi zony)*. Nauka, Novosibirsk, 214 pp (in Russian).
- Kanygin A.V., Moskalenko T.A., Jadrenkina A.G. and Semenova V.S., 1977. *On Stratigraphic Sectioning and Correlations of Middle Ordovician Siberian Platform. Stratigraphic Problems of Ordovic and Silur in Siberia (O stratigraficheskom raschlenenii i korreliatsii srednego ordovika Sibirskoi platformy. Problemy stratigrafii ordovika i silura Sibiri)*. Nauka, Novosibirsk, 3–43 (in Russian).
- Kent D.V. and Smethurst M.A., 1998. Shallow bias of paleomagnetic inclinations in the Paleozoic and Precambrian. *Earth Planet. Sci. Lett.*, **160**, 391–402.
- Kent D.V., Briden J.T. and Mardia K.W., 1983. Linear and planar structure in ordered multivariate data as applied to progressive demagnetisation of paleomagnetic remanence. *Geophys. J. R. Astron. Soc.*, **75**, 593–621.
- Khranov A.N., Rodionov V.P. and Komissarova R.A., 1965. New data on Paleozoic history of the Earth's magnetic field on the territory of SSSR (Novye dannye o paleozoiskoi istorii zemnogo magnitnogo polya na territorii SSSR). In: *Present and Past Magnetic Fields of the Earth (Nastoyashchee I proshloe magnitnogo polya Zemli)*. Nauka, Moscow, 206–213 (in Russian).
- Khranov A.N., Goncharov G.I., Komissarova R.A., Pogarskaya I.A., Rodionov V.P., Slaytsitais I.P., Smirnov L.S. and Forsh N.N., 1974. *Paleozoic Paleomagnetism (Paleomagnetism paleozoya)*. Nedra, Leningrad, 236 pp. (in Russian).
- Khranov A.N. and Rodionov V.P., 1977. Problem of Laurasia in Early and Middle Paleozoic in the light of paleomagnetic data (Problema Lavrasii v rannem I srednem paleozoe v svete paleomagnitnykh dannykh). In: *Paleomagnetism and Problems of Plate Tectonics (Paleomagnetism i voprosy tektoniki plit)*, Trudy VNIGRI, **394**, 108–140 (in Russian).
- Khranov A.N. and Rodionov V.P., 1980. The geomagnetic field during Paleozoic time. *J. Geomagn. Geoelectr.*, **32**, Suppl III, 99–115.
- Khranov A.N., 1988. Components of the natural remanent magnetisation of sedimentary rocks and their reference to magnetostratigraphy. In: *Magnetostratigraphy and Paleomagnetism of Sedimentary and Volcanic Formations of SSSR (Magnitostratografiya i paleomagnetism osadochnykh i vulkanogennykh formatsyi SSSR)*. VNIGRI, Leningrad, 85–96 (in Russian).
- Kirschvink J.L., 1980. The least-squares line and plane and the analysis of paleomagnetic data. *Geophys. J. Astron. Soc.*, **62**, 699–718.
- Krijgsman W., Delahaije W, Langereis C.G. and de Boer P.L., 1997. Cyclicity and *NRM* acquisition in a continental red bed sequence (Miocene, Spain): potential for an Astronomical Polarity Time Scale. *Geophys. Res. Lett.*, **24**, 1027–1030.
- Kruiver P.P., Dekkers M.J. and Langereis C.G., 2000. Secular variation in Permian red beds from Dôme de Barrot, SE France. *Earth Planet. Sci. Lett.*, **179**, 205–217.
- Kruiver P.P., Dekkers M.J. and Heslop D., 2001. Quantification of magnetic coercivity components by the analysis of acquisition curves of isothermal remanent magnetization. *Earth Planet. Sci. Lett.*, **189**, 269–276.

- Kruiver P.P., Langereis C.G., Krijgsman W. and Dekkers M.J., 2002. Cyclostratigraphy and rock-magnetic investigation of the *NRM* signal in late Miocene palustrine-alluvial deposits of the Librilla section (SE Spain). *J. Geophys. Res.*, **107(B12)**, doi:10.1029/2001JB000945.
- Nikiforova O.U. and Andreeva O.N., 1961. *Stratigraphy of Ordovician and Silurian Siberian Platforms and Their Paleontologic Reasoning (Stratigraphiya ordovika i silura sibirskoi platformy i ee paleontologicheskoe obosnovanie)*. Gostoptekhizdat, Leningrad, 412 pp. (in Russian).
- Ogienko L.V., 1992. Trilobites and biostratigraphy of Lower Ordovician sediments on the south of Siberian Platform (Trilobity i biostratigraphija nizhneordovikskikh otlozhenii na yuge Sibirskoi platformy). Nedra, Moscow, 145 pp. (in Russian).
- Pavlov V.E., Rodionov V.P., Khramov A.N. and Gallet Y., 1999. Magnetostratigraphy of the Polovinka key section, Midstream Lena River: Did the geomagnetic polarity change in the Early Llandeilian? *Fizika Zemli*, **5**, 61–71 (in Russian).
- Pesonen L.J. and Halls H.C., 1983. Geomagnetic field intensity and reversal asymmetry in late Precambrian Keweenawan rocks. *Geophys. J. Roy. astron. Soc.*, **73**, 241–270.
- Roberts D.H., Lehar J. and Dreher J.W., 1987. Time series analysis with clean. I. Derivation of a spectrum. *Astron. J.*, **93**, 968–989.
- Rodionov V.P., 1966. On dipole character of the Earth's magnetic field in Late Cambrian and Ordovician on the south of Siberian Platform (O dipol'nosti Zemnogo magnitnogo polia v pozdnem kembrii i ordovike na yuge Sibirskoi platformy). *Geologiya i geofizika*, **1**, 94–101 (in Russian).
- Rodionov V.P. and Osipova E.P., 1985. Regional paleomagnetic scale of the Lower Palaeozoic of the Siberian platform. In: *Stratigrafiya pozdnego dokembriya i nizhnego paleozoya Sibirskoi platformy*. Leningrad, VNIGRI, 65–76.
- Rodionov V.P., Pavlov V.E. and Gallet Y., 2001. Magnetic polarity structure of the Stratotype section of the Mid Ordovician Kirenskii-Kudrinskii and Chertovskii horizons (up the Lena River, above the Town of Kirensk) in relation to the Ordovician Geomagnetic superchron. *Physics of the Solid Earth (Izvestiya)*, **37**, 498–502.
- Siberian Stratigraphic Resolution Committee, 1983. Resolutions of All Union Stratigraphic Conference on Precambrian, Lower Paleozoic and Quarternary of middle Siberia. Part 1. (Upper Proterozoic and lower Paleozoic). (Resheniya Vsesoyuznogo stratigraficheskogo soveshchaniya po dokembriyu, paleozoyu i chetvertichnoi sisteme srednei Sibiri. Chast' 1. (Verkhniy proterozoi i nizhniy paleozoi). Novosibirsk, 1983, 216 pp. (in Russian).
- Sokolov B.S. and Tesakov Yu.I. (Eds), 1975. *Ordovician Stratigraphy of the Siberian Platform*. Nauka, Siberian branch, Novosibirsk, pp. 214 (in Russian).
- Torsvik T.H., Tait J., Moralev V.M., McKerrow W.S., Sturt B.A. and Roberts D., 1995. Ordovician paleogeography of Siberia and adjacent continents. *J. Geol. Soc. London*, **152**, 279–287.
- Van der Voo R. and Torsvik T.H., 2001. Evidence for late Paleozoic and Mesozoic non-dipole fields provides an explanation for the Pangea reconstruction problems. *Earth Planet. Sci. Lett.*, **187**, 71–81.
- Zijderveld J.D.A., 1967. A.C. Demagnetization of rocks: analysis of results. In: D.W. Collinson (Ed.), *Methods in Palaeomagnetism*, Elsevier, Amsterdam, 254–286.